Life-Cycle of Structures and Infrastructure Systems – Biondini & Frangopol (Eds)

Dynamic assessment of a stress-ribbon CFST arch bridge with SHM and NDE

J.P. Huang, L.Q. He, J.Q. Xue, S.N. Zhou & B. Briseghella
Sustainable and Innovative Bridge Engineering Research Center & Joint International Research Laboratory of Deterioration and Control of Costal and Marine Infrastructures and Materials, College of Civil Engineering, Fuzhou University, Fuzhou, China

C. Castoro & A. Aloisio
Department of Civil, Construction-Architectural and Environmental Engineering, University of L'Aquila, L'Aquila, Italy

G.C. Marano
Department of Structural, Environmental and Geotechnical Engineering, Polytechnic University of Turin, Turin, Italy
Joint International Research Laboratory of Deterioration and Control of Costal and Marine Infrastructures and Materials, College of Civil Engineering, Fuzhou University, China

ABSTRACT: Vibration-based structural health monitoring is an efficient technique for dynamic assessment of the structures. Based on the identified dynamic characteristics, the condition of a bridge can be assessed by means of structural identification through the finite element model updating procedure. The modal parameters are generally the indicators that reflect the changes of the global performance of the bridges. As the supplement, non-destructive evaluation methods can be employed to provide more detailed information about the local condition of the structure. In this study, operational modal analysis was performed on a butterfly-arch pedestrian bridge at Fuhzou Univesity, which was based on an innovative design concept, known as the stress-ribbon bridge. The uncertain model parameters of the structure were identified by updating the refined FE model in reference to the experimental modes. The ultrasonic instruments and rebound hammers were used to determine the debonding condition of the concrete-filled steel tubular sections of the main arches and the elastic modulus of the concrete slabs, respectively. Both of them play an important role to influence the dynamic behaviour of the bridge. The key structural parameters that were identified by the FE model updating procedure are compared to the nondestructive testing results. It's found that the nondestructive testing methods provide important supplementary information to the SHM for condition assessment of the structure.

1 INTRODUCTION

In vibration-based structural health monitoring (VBM), operational modal data is usually extracted by ambient vibration tests (AVT) to investigate the initial state of the bridges and structures. On the basis, the baseline model can be built by model calibration for long-term monitoring of the structure with good accuracy and high fidelity. The modal information (e.g., natural frequencies and mode shapes) are however the indicators of global dynamic characteristics of the structure, which sometimes have difficulties to reflect minor structural degradation or localized deterioration of the materials (Aktan et al. 2000). On the other hand, non-destructive evaluation (NDE) technique focuses on the local condition of the structures. Verma et al. (2013) provided a comprehensive review of nondestructive testing methods for condition monitoring of concrete structures. It's concluded that NDE methods have been used for more than three decades for monitoring concrete structures, which has currently

DOI: 10.1201/9781003323020-336

reached a mature status for condition evaluation of existing RC structures. However, as the local approach of structural evaluation the application of the NDE on site can be very time-consuming and require heavy labour works. The advantages and disadvantages of the SHM and NDE suggest that both approaches can be supplementary to each other. Aldrin et al. (2016) presented a comprehensive approach that integrates the VBM and NDE under the framework of probability of detection (POD) evaluation procedure for aerospace structures. By using a model-based method, they discovered that justification of the underlying assumptions of the statistical model choices was the key to the success of condition-based maintenance for the real applications. In this regard, development of a comprehensive approach of SHM and NDE is highly anticipated by civil engineers. Patil & Reddy (2020) presents a combination of the vibration-based method and non-destructive method for damage assessment of carbon composite fiber reinforced structure. Changes of the frequency response functions are used as the damage indicator to distinguish the intact and damaged specimens. Following that, the ultrasonic C-scanning method is used to locate and quantify the damage in the specimen. Vandecruys et al. (2022) presents a case study of acoustic emission and vibration-based monitoring of locally corroded reinforced concrete beams. Their findings suggested that the local (NDE) and global (VBM) monitoring techniques supplemented each other. The proposed comprehensive approach increased the sensitivity and efficiency of damage detection method in different phases of corrosion damage progress.

In the current study, an onsite investigation of an arch pedestrian bridge is performed by using VBM and NDE. The current study follows a previous research work on the same structure (He et al. 2022). The local defects of the main arches, known typically as debonding/void of the concrete core is the focus of the current work. Ultrasonic testing was implemented to assess the condition of the Concrete-Filled Steel Tubular (CFST) composite sections. In addition, the deck system of the bridge, known as the stress ribbon, is composed of several precast concrete segments. Evaluation of the compressive strength and hardness of the concrete slab is conducted by the rebound hammer testing. The results of structural identification obtained by the FE model updating method are then presented. Fidelity of the updating results will be addressed in reference to the findings of NDE for the identified model parameters.

2 EXPERIMENTAL PROGRAM

2.1 *Description of the bridge*

As shown in Figure 1, the stress-ribbon deck of the pedestrian bridge is supported by the cross beams between the outward inclined CFST arches, also known as the butterfly arches. Since the stress ribbons were anchored to the abutment where the springs of the arches were rooted, the whole structure consists of the self-anchored system, which loads the foundations mainly in the gravity direction. The span of the main arches is 25 meters with the rise of 5.5 meters. See Figure 2. They are made of the 42.6cm-diameter steel pipes with the thickness of 1.6 cm. The angel between the inclined arches and the ground is 60 degrees. The span of the secondary arches is 16.8 meters. They are made of the 37.7cm-diameter steel pipes with the thickness of 1.6 cm. The connections between the main and the secondary arches are welded. They are also interconnected by seven rigid hangers on each side. The stress-ribbon deck was assembled from the precast concrete segments by using two pre-stressed tendons. Each of the precast segment is 6 meters in width, 1.15 meters in length and 14 cm in thickness. The tendons are formed by two bundles of 12×Φ15.2mm monostrands grouted inside the galvanized steel pipes. The middle part of the bridge deck simply rests on the cross beams, whereas the side parts of the bridge deck are supported by the pre-stressed tendons. See Figure 3.

2.2 *Ultrasonic testing*

2.2.1 *Working principle*

Debonding is the common structural defect of the CFST members in an arch bridge (Chen et al. 2022). They can usually be assessed by using the ultrasonic testing method. Shown in Figure 4 is a typical sound wave transmission detector for quality testing of the CFST construction.

Figure 1. A stress-ribbon CFST arch pedestrian bridge at Fuzhou university.

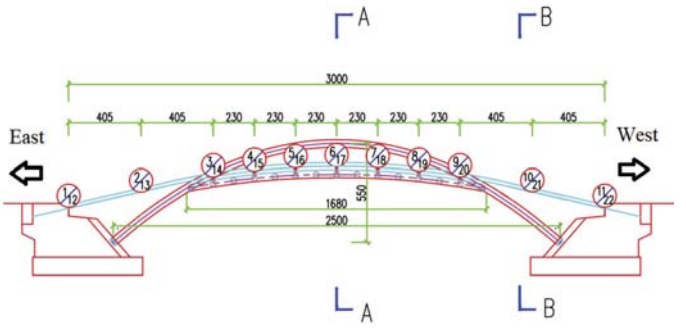

Figure 2. Front view of the bridge with the measurement nodes of AVT labeled (units in mm).

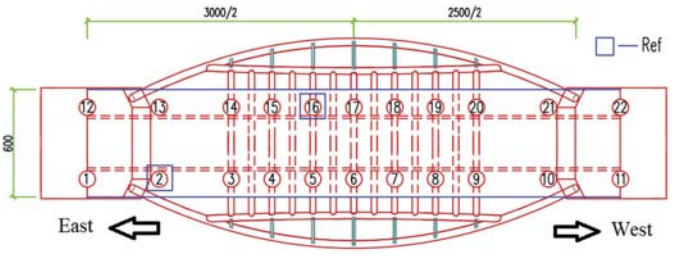

Figure 3. Top view of the bridge with the measurement nodes of AVT labeled (units in mm).

The propagation speed of ultrasonic waves in solid is a function of the Young's modulus E and the density ρ of the materials, $V_{solid} = f(E/\rho)$. The ultrasonic wave speed in steel and concrete is generally 4000–6000 m/s (Li et al. 2020). Under a certain ambient condition, the following relationship applies for the ultrasonic wave speeds,

$$\frac{V_S}{V_C} = p_c \tag{1}$$

where V_s = the wave speed in steel; V_c = the wave speed in concrete; and p_c = a constant to be determined. For a CFST section without defects, the ultrasonic time-of-flight T_f equals to,

$$T_f = \frac{2 \cdot t}{V_S} + \frac{D - 2 \cdot t}{V_C} \tag{2}$$

where t = the thickness of steel pipe; D = the diameter of steel pipe. Once p_c is obtained by the CFST specimen tests, both V_s and V_c can be obtained by solving Equation (2). On the basis, for the CFST sections with debonding/void, the ultrasonic time-of-flight T_f can be estimated by

Figure 4. Ultrasonic instrument: WE-520 sound wave transmission detector (operating at 50 kHz).

$$T_f = \frac{2 \cdot t}{V\mathrm{s}} + \frac{D - 2 \cdot t - \Delta h}{V\mathrm{c}} + \frac{\Delta h}{V\mathrm{a}} \tag{3}$$

where Δh = the thickness of void or debonding in the concrete core on the path of the wave passage and V_c = the wave speed in air, which can be assumed as a constant of 340m/s.

2.2.2 *Testing scheme*

As shown in Figure 5, on each cross section of the CFST the ultrasonic tests were repeated in four different directions. They were equally distributed around the perimeter and all go through the center of the cross section. The values of the ultrasonic time-of-flight T_f were read from the device. And the thickness of debonding Δh can be determined by Equation (3). A linear interpolation is then applied to the discrete values of Δh along the perimeter of the section to estimate the total debonding area at the concrete core. On the main arches, eleven cross sections were tested at each side. See Figure 6. In addition, before the ultrasonic testing, the traditional testing method of hammer impacts was also applied in order to quickly evaluate the severity of the debonding condition. The results of the hammer impact tests were indicated by the quality number N_q. For instance, N_q=10 for the arc-length ratio of debonding R_d < 5%, N_q=9 for R_d = 5~10%, N_q=8 for R_d = 10~20%, and N_q=7 for for R_d = 20~30% (Xue et al. 2012).

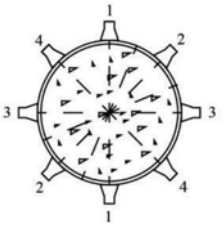

Figure 5. Placement of the probes at the cross section in the ultrasonic testing.

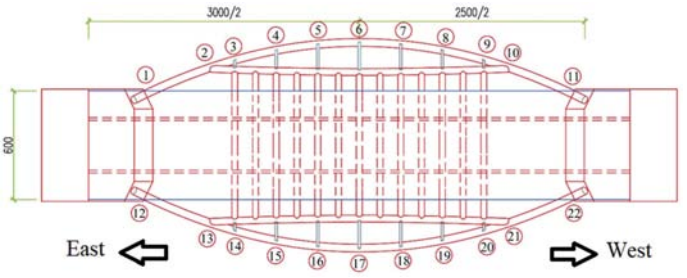

Figure 6. Top view of the bridge with the cross sections of ultrasonic testing labeled (units in mm).

2.3 *Rebound hammer testing*

2.3.1 *Working principle*

A rebound hammer is a handheld device for non-destructive testing of concrete. It helps determine the compressive strength and hardness of concrete by measuring the rebound height of a steel ball dropped onto the surface. The relevant technical specification (MOHURD 2011) in China provides the detailed requirements and process to perform the rebound hammer testing. In particular, the depth of the carbonation at the concrete surface has to be identified, which influences the results of the rebound hammer tests. To convert the cubic strength of concrete $f_{cu,k}$ to the corresponding Young's modulus of concrete $E_{c,s}$, the Chinese Code for design of concrete structure (MOHURD 2015) suggests the following formula:

$$E_{\mathrm{c,s}}=\frac{10^5}{2.2+\frac{34.7}{f_{cu,k}}}\,(\mathrm{MPa}) \tag{4}$$

The values *Ec,s* above are however the static elastic modulus of concrete. Memory et al. (1995) suggests the following equation to calculate the dynamic elastic modulus of concrete *Ec,d*:

$$E_{\mathrm{c,s}}=1.25E_{\mathrm{c,d}}-19(\mathrm{GPa}) \tag{5}$$

2.3.2 *Testing scheme*

Since the concrete deck is fully covered with the ceramic pavement, the rebound hammer tests were only applied from underneath the bridge. By considering the accessibility, the two segments of the precast concrete slab next to the east and west abutments were tested.

2.4 *Ambient vibration testing*

Ambient vibration tests were performed for twenty-two measurement nodes distributed on the bridge deck across the span. The acquisition system consisted of four wireless accelerometers. The signals of three-dimensional records were highly synchronized. As shown in Figure 3, the nodes No. 2 and No. 16 were the reference nodes, which are used to glue the separate mode shape vectors from each individual testing setups. In detail, the tests included 11 setups.

System and modal parameters are extracted from the ambient data with the output-only reference-based stochastic subspace identification algorithm (Peeters et al. 1999). The reference channels were those of the reference sensors. Data processing and system identification process was accomplished by using the MACEC toolbox (Reynders et al. 2014).

3 EXPERIMENTAL RESULTS

3.1 *Ultrasonic testing*

By the tests of the CFST specimens in laboratory, p_c in Equation (1) is found to be 1.18. Correspondingly, V_s = 7,778 m/s and V_c = 4,896 m/s by solving Equation (2). On the basis of the working principle in Section 2.2.1, the debonding/void rate k_d can be obtained, which defines the ratio between the debonding/void area and the circular area of the concrete core at the CFST cross section. On the basis of the formulas to calculate the design values of the compressive and flexural stiffness of the CFST members (Chen et al. 2022), the following equation is proposed herein for the equivalent stiffness of the CFST members:

$$(EA)'_{\mathrm{equivalent}}=E_{\mathrm{s}}A_{\mathrm{s}}+kE_{\mathrm{c}}A_{\mathrm{c}} \tag{6}$$

$$(EI)'_{\mathrm{equivalent}}=E_{\mathrm{s}}I_{\mathrm{s}}+0.6kE_{\mathrm{c}}I_{\mathrm{c}} \tag{7}$$

where the subscripts *s* and *c* stand for the steel pipe and concrete core, respectively. The reduction factor of 0.6 to the flexural stiffness of the concrete core E_cI_c takes into account the cracking of the concrete core under tension (Chen et al. 2022). By considering the effects of debonding, the

values of the compressive and flexural stiffness of the CFST section can be modified by introduction of the reduction factor k (= 1-k_d). The experimental results of the ultrasonic testing are given in Figure 7 in terms of the k factors. The mean values of k are similar of the two main arches, around 0.98. The minimum values of k are found at the springs of the arches, around 0.97. In particular, the experimental results obtained from the ultrasonic testing are usually in agreement with the findings of the hammer impact tests. The crown sections are labeled by 10, suggesting an almost zero debonding rate. And the spring sections are labeled by N_q=7, suggesting the most severity of the debonding condition.

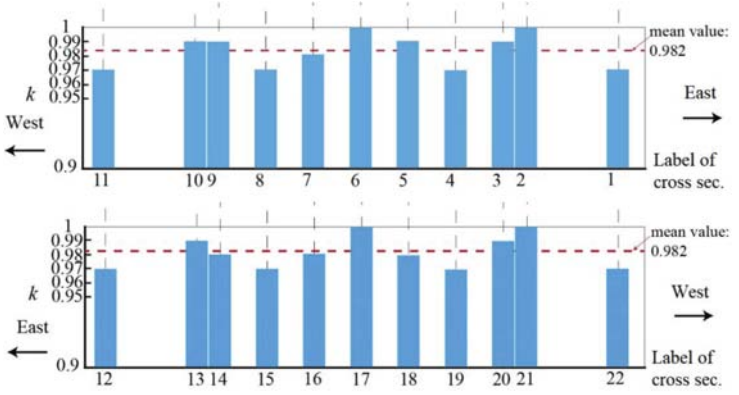

Figure 7. Stiffness reduction factors k identified at the CFST cross sections by ultrasonic testing.

3.2 *Rebound hammer testing*

Totally 16 rebound hammer tests shall be repeated on an individual test area (MOHURD 2011). In Table 1, the results of the hammer tests are provided in detail. The two deck segments being tested are, repetitively, next to the east and west abutments. The cubic strength of the concrete was obtained in reference to the specification. The static elastic modulus of concrete $E_{c,s}$ is then estimated by Equation (4). Finally, the dynamic elastic modulus of concrete $E_{c,d}$ is obtained by Equation (5). Figure 8 illustrates the variation of the rebound values on each test area for the 4 by 4 test points in the gray colour scale.

Table 1. Results of rebound hammer testing.

Test area	Rebound value (mm)				Average value (mm)	Carbonization depth (mm)	Cubic strength (MPa)	Static $E_{c,s}$ (MPa)	Dynamic $E_{c,d}$ (MPa)
East	52	52	58	49	54.1	3.0	57.8	35,709	43,767
side	56	42	57	57					
	54	58	54	46					
	56	56	52	52					
West	44	45	36	47	45.4	1.5	46.6	33,960	42,372
side	46	48	39	46					
	42	46	48	45					
	52	63	44	54					

3.3 *Ambient vibration testing*

The results of the ambient vibration tests were provided in Table 2 concerning the identified experimental modes. They included five vertical bending modes and three torsion modes. No lateral modes were identified under the current ambient vibration conditions. The identified damping ratios were generally around 1% except of the second mode. Significant modal deformation was observed in the 2nd mode for the main arches, whereas the other bending or torsion modes were

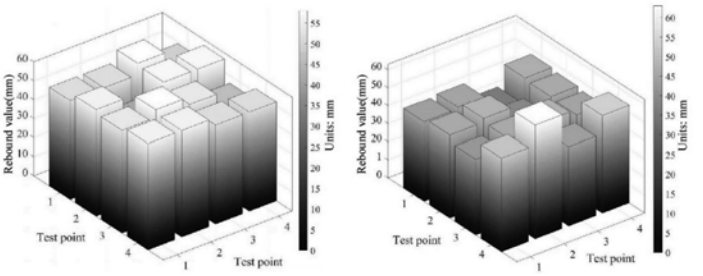

Figure 8. Rebound values at the slabs of the west side (left) and east side (left).

characterized with the deformation mainly for the slab. The composite action of CFST cross sections is considered to influence the energy dissipation mechanism for the the 2nd vibration mode.

Table 2. The identified experimental modes.

No.	Nature frequency f (Hz)	Damping ratio ξ	Type of the vibration modes
1	3.59	0.7%	1st Vertical bending mode
2	5.28	3.9%	2nd Vertical bending mode
3	6.91	1.6%	1st Torsion mode
4	7.79	1.2%	3rd Vertical bending mode
5	9.17	1.1%	2nd Torsion mode
6	10.98	1.0%	3rd Torsion mode
7	14.45	0.8%	4th Vertical bending mode
8	14.92	0.6%	5th Vertical bending mode

4 RESULTS OF MODAL-BASED FE MODEL UPDATING

Structural identification was performed by using parametric updating of the refined reference model of the bridge (He et al. 2022). In the refined FE model, the bridge deck was modeled with the shell elements. Four rigid links were introduced between the anchors of the prestressed tendons and the springs of the main arch to simulate the abutments. The numerical solution process of the FE model updating was formulated into the nonlinear least square problem, which intends to minimize the relative differences between the experimental and numerical natural frequencies. The stiffness of the soil springs at the abutments, the elastic modulus of the concrete deck E_c and the elastic modulus of the tendons E_t were chosen as the updating parameters for a total of eight parameters. Under the optimal solution, E_C of the concrete deck is identified as 57,598 MPa. E_C of the concrete core of the CFST sections is 42,000 MPa and the E_S of the steel pipe of CFST is 210,000 MPa. In particular, both of them were not included into the updating parameters and kept as the constants in the updating process.

5 DISCUSSION

The results of ultrasonic testing show that the average debonding/void rate k_d is 2% for all the 22 cross sections along the main arches. Xue et al. (2012) found that if the debonding/void rate k_d is less than 1.2%, its influence on the ultimate load capacity and stiffness of CFST columns can be neglected. Therefore, for the current CFST bridge, it might be necessary to consider the uncertainty of E_C of the concrete core of the CFST main arches by taking it as one of the updating parameters. In addition, with respect to the variation of k (Figure 6), the assumption for a uniform value of E_C for the main arches is acceptable. Besides, both hammer impact tests and ultrasonic tests found almost zero debonding rate on the secondary arches. Therefore, the stiffness of the secondary arches need not be updated, since the initial estimation of the material properties are sufficiently accurate.

The results of rebound hammer testing showed the variation of E_C of the concrete deck between the selected two segments. The absolute value of the relative difference is 3.2%. In this regard, it is reasonable to assume a constant E_C of the concrete deck in the FE model updating. The identified value by FE model updating is found to be almost 30% greater than those identified by NDE. The non-structural elements, including the hand-rails and ceramic pavement should contribute to the increased value of E_C., as well as the influence of pre-stressing forces at the tendons. Nevertheless, further investigation remains open for any future research.

6 CONCLUSION

In this study, a butterfly-arch pedestrian bridge was investigated by both VBM and NDE methods. The uncertain model parameters of the structure were identified by updating the refined FE model in reference to the experimental modal data. The ultrasonic instruments and rebound hammers are used to determine the debonding condition of the CFST members of the main arches and the elastic modulus of the concrete slabs, respectively. Both of them play an important role to influence the dynamic performance of the self-anchored structural system. Accuracy and variability of the key structural parameters that were identified by the FE model updating process is investigated in comparison to the NDE results. It is found that the NDE methods serve as an important supplementary technique to the SHM technique for condition assessment of the studied structure.

REFERENCES

Aktan, A.E., Catbas, F.N., Grimmelsman, K.A. & Tsikos, C.J. 2000. Issues in infrastructure health monitoring for management. *Journal of Engineering Mechanics*, 126(7): 711–724.

Aldrin, J.C., Annis, C., Sabbagh, H.A. & Lindgren, E.A. 2016, February. Best practices for evaluating the capability of nondestructive evaluation (NDE) and structural health monitoring (SHM) techniques for damage characterization. *42ND ANNUAL REVIEW OF PROGRESS IN QUANTITATIVE NONDESTRUCTIVE* EVALUATION: *Incorporating the 6th European-American Workshop on Reliability of NDE*. AIP Publishing LLC.

Chen, B., Liu, J. & Wei, J. 2022. *Concrete-Filled Steel Tubular Arch Bridges*. Beijing: China communication press: Springer.

Ministry of Housing and Urban-Rural Development of the People's Republic of China (MOHURD). 2015. *Code for design of concrete structures*. Beijing: China Architecture & Building Press.

He, L., Castoro, C., Aloisio, A., Zhang, Z., Marano, G.C., Gregori, A., Deng, C. & Briseghella, B. 2022. Dynamic assessment, FE modelling and parametric updating of a butterfly-arch stress-ribbon pedestrian bridge. *Structure and Infrastructure Engineering* 18: 1–12.

Ministry of Housing and Urban-Rural Development of the People's Republic of China (MOHURD). 2011. *Technical specification for inspecting of concrete compressive strength by rebound method*. Beijing: China Architecture & Building Press.

Li, H., Yan, P., Sun, H. & Yin, J. 2020. Axial compression performance and ultrasonic testing of multicavity concrete-filled steel tube shear wall under axial load. *Advances in Civil Engineering*, 2020(1): 1–19.

Memory, T.J., Thambiratnam, D.P. & Brameld, G.H. 1995. Free vibration analysis of bridges. *Engineering Structures*, 17(10): 705–713.

Patil, S. & Reddy, D.M. 2020. Impact damage assessment in carbon fiber reinforced composite using vibration-based new damage index and ultrasonic C-scanning method. *Structures* 28: 638–650.

Peeters, B. & De Roeck, G. 1999. Reference-based stochastic subspace identification for output-only modal analysis. *Mechanical systems and signal processing* 13(6): 855–878.

Reynders, E., Schevenels, M. & De Roeck, G. 2014. *MACEC 3.3: A Matlab Toolbox for Experimental and Operational Modal Analysis*. Katholieke Universitieit: Leuven.

Vandecruys, E., Martens, C., Van Steen, C., Nasser, H., Lombaert, G. & Verstrynge, E. 2022. Preliminary results on acoustic emission and vibration-based monitoring of locally corroded reinforced concrete beams. *The International Symposium on Nondestructive Testing in Civil Engineering* 27

Verma, S.K., Bhadauria, S.S. & Akhtar, S. 2013. Review of nondestructive testing methods for condition monitoring of concrete structures. *Journal of construction engineering* 2013(2008): 1–11.

Xue, J.Q., Briseghella, B. & Chen, B.C 2012. Effects of debonding on circular CFST stub columns. *Journal of Constructional Steel Research* 69(1): 64–76.